Accepted Manuscript

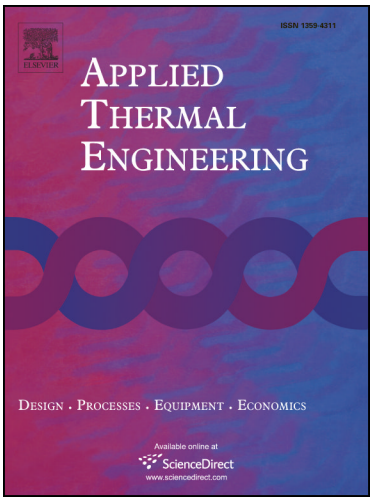

Positive Impact of a Tower Inlet Cover on Natural Draft Dry Cooling Towers Under Crosswind Conditions

Quanlong Liu, Lin Xia, Mengqi Hu, Xiaoxiao Li, Zihao Mi, Junjie Jia

PII: S1359-4311(17)37720-7
DOI: https://doi.org/10.1016/j.applthermaleng.2018.04.129
Reference: ATE 12126

To appear in: *Applied Thermal Engineering*

Received Date: 5 December 2017
Revised Date: 31 March 2018
Accepted Date: 26 April 2018

Please cite this article as: Q. Liu, L. Xia, M. Hu, X. Li, Z. Mi, J. Jia, Positive Impact of a Tower Inlet Cover on Natural Draft Dry Cooling Towers Under Crosswind Conditions, *Applied Thermal Engineering* (2018), doi: https://doi.org/10.1016/j.applthermaleng.2018.04.129

Positive Impact of a Tower Inlet Cover on Natural Draft Dry Cooling Towers Under Crosswind Conditions

Quanlong Liu [1], Lin Xia [2,*], Mengqi Hu[2], Xiaoxiao Li [3,*], Zihao Mi[2], Junjie Jia[4]

[1] School of Management, China University of Mining & Technology, Xuzhou, China

[2] Xi'an Thermal Power Research Institute Co. Ltd, Xi'an, China

[3] School of Mechanical and Mining Engineering, the University of Queensland, Bribane, Australia

4 Qinghai New Energy Intergration Co. Ltd of Huanghe Hydropower, Xining, China

Correspondence should be addressed to Lin Xia (xialin@tpri.com.cn) and Xiaoxiao Li (x.li3@uq.edu.au)

Abstract

This study proposes a tower inlet cover to improve the performance of the small natural draft dry cooling tower (NDDCT) under crosswind conditions. CFD analyses are performed on a small NDDCT with tower inlet covers of different lengths, and the CFD model is validated against experimental results. The air temperature, air pressure, air flow and heat flux fields are presented, and the thermal performance for each heat exchanger and the NDDCT are obtained using CFD simulations. The CFD simulation results show that the high-pressure zone around the tower side wall, formed by the crosswind, causes the decrease in air flow through the tower and the deterioration in tower performance with a crosswind. The tower inlet cover can improve the tower performance in crosswinds by increasing the air flow of the heat exchangers. Tower inlet covers with lengths of 1.5 m, 3 m and 4.5 m improve the tower heat load by 40% to 65%, 70% to 130% and 85% to 230%, respectively, when the crosswind increases from 4 m/s to 12 m/s.

Keywords: natural draft dry cooling tower; numerical simulation; crosswind;

1. Introduction

Cooling towers are commonly used in large thermal systems, such as industrial power generation units, refrigeration and air conditioning plants, chemical and petrochemical industries to dissipate process heat. Different types of cooling towers are

distinguished from each other by different criteria. Cooling tower is either mechanical draft type or natural draft type based on the method used to move the air through the system [1].

For the mechanical draft cooling tower, many researchers have investigated the improvement method of its performance. Lemouari et al. [2] presented an experimental investigation of the thermal performances of a mechanical draft cooling tower filled with a "VGA" (Vertical Grid Apparatus) type packing. Two operating regimes were observed to determine the best way to promote the heat transfer. Singh and Das [3] proposed a feedback model in order to control the performance of a mechanical draft cooling tower under varying heat load conditions suiting diverse applications such as solar power generation, HVAC and diesel engine. By monitoring the inlet water temperature with time, the controlling variable governed by water to air ratio has been adjusted to optimize the tower operation. Singh and Das [4] also proposed a constrained multiple parameter inverse identification technique for a mechanical cooling tower to meet a required heat rejection rate from hot water and also ensuring minimum power consumption. The technique minimizes the relevant objective function involving the total power consumption satisfying the constraint of the required heat load in the inverse analysis.

Based on the different ways of heat transfer, the natural draft cooling tower could be divided into the natural draft wet cooling tower (NDWCT) and the natural draft dry cooling tower (NDDCT). In a NDWCT, heat is mainly transferred by latent heat transfer through water, which improves the performance of the cooling water system [5]. However, large quantities of water evaporate into the moving air stream. Williams and Rasul [6] reported that the water evaporation rate of a power plant with a capacity of 350 MW in Queensland, Australia was approximately 1.8 litres of water per kWh of power generated. Gurgenci [7] also predicted that the total water consumption rate for a geothermal power plant was approximately 0.4 kg/s per MW of heat rejected. In contrast, heat is dissipated by only convective heat transfer in a NDDCT. This feature is advantageous for water conservation. Thus, the NDDCT becomes a competitive option for many power plants located in arid places due to water consumption restrictions. Xia et al. [8] compared the annual water consumption of a NDWCT and that of a NDDCT in a 300 MW power plant and found that the power plant could reduce its water consumption

by approximately 5 million tons of water per year by replacing a NDWCT with a NDDCT.

Although the NDDCT is the competitive option for a power plant located in arid places, it still faces two considerable challenges; specifically, the hot ambient temperature and crosswinds both have negative effects on cooling performance [9]. The thermal performance of the NDDCT depends principally on the entering air-dry bulb temperature [8], while that of the NDWCT depends principally on the entering air-wet bulb temperature [10]. Thus, a power plant employed with the NDDCT would suffer higher condenser pressure and lower power production than the power plant employed with the NDWCT, for the same ambient temperature and operation conditions [8]. The impact on the revenue of the plant employed with the NDDCT is even higher since these high ambient temperature periods represent peak power demand for most locations [11]. In this case, several approaches have been developed to address these problems. Several inlet air pre-cooling methods, such as spray cooling [12-14] and wetted-media cooling [15-17], have been developed to improve the NDDCT's performance during the high ambient temperature period. Spray cooling has become increasingly used due to its simplicity, low capital cost and ease of operation and maintenance [14]. Different from ambient temperature, crosswind causes a significant decrease in performance by disturbing the natural draft processes, and its effects are considerably more complex and difficult to predict. Du Preez and Kroger [18] used a numerical procedure to investigate the influence of the arrangement of heat exchangers on the performance of a tower in windy conditions and verified the results via full-scale and experimental measurements. The results indicated that the arrangement of heat exchangers and windbreak walls may considerably reduce the adverse effect of crosswind on the performance of dry cooling towers. Al-Waked and Behnia [19] conducted a three-dimensional study of the impact of the location and porosity of windbreak walls on a NDDCT by using the standard k-ε model. The results indicated that introducing windbreak walls could improve the thermal performance of the NDDCT. Optimizing the location of the windbreak walls was shown to have a more significant effect on the NDDCT thermal performance than the porosity of the walls. Goodarzi proposed a new tower exit configuration [20], radiator-type windbreakers [21] and an alternative tower shell geometry with an elliptical cross section

[22] to improve the cooling efficiency of NDDCTs in crosswinds. Yang et al. [23] investigated the performance of an indirect dry cooling system by coupling the simulated thermos-hydraulic performances of the air-cooled heat exchanger and cooling tower with condenser performance. Each cooling delta of the air-cooled heat exchanger was modelled precisely according to its geometric details; thus, the dimensional characteristics of flow and heat transfer of cooling deltas and sectors could be obtained. The simulation results showed that the performance of upwind cooling deltas is superior to those in the rear and on the side. Chen et al. [24] investigated improving performance via interior and exterior windbreaker configurations to propose measures mitigating the adverse effects of crosswind. His study showed that the exterior windbreakers outperform the interior ones in terms of thermo-flow performance. Ma et al. [25] optimized setting angles of wind-break walls to get larger cooling performance enhancement for NDDCT with vertical cooling deltas under crosswind. Wang et al. [26] reconstructed the destructed inlet flow field with a labyrinth structure based on the influencing mechanisms of the crosswind. The numerical results revealed that the proposed flow field reconstruction approach increase the ventilation rate of a NDDCT by 62% under high speed crosswind conditions. Kong [27] proposed an annularly arranged air-cooled condenser for NDDCT to improve thermo-flow performances.

Small NDDCTs suffer more from crosswind impact than large NDDCTs. Lu et al. [28] conducted CFD modelling to numerically analyse the heat transfer performance of a 15-m-high small NDDCT with different crosswind speeds. His simulation results showed that a crosswind degrades cooling performance significantly at certain crosswind speeds. However, the negative effect of a crosswind can be made positive in small NDDCTs by introducing windbreak walls that guide the air mobilized by crosswinds through the heat exchangers. Lu et al. [29] also investigated the influence of windbreak wall orientation on the cooling performance of small NDDCTs. The simulation results indicated that the tri-blade-like walls should be placed with one wall, i.e., one axis of symmetry, always aligned with the dominant crosswind direction. Li et al. [30] proposed a new method to increase the performance of a small NDDCT in crosswinds by optimizing the hot water mass flow rate in air-cooled heat exchangers. His results showed that this method increases the cooling performance of the NDDCT by 18% when the crosswind speed is 4

m/s. They also [31] [32] developed the experimental studies on a 20 m high NDDCT. They presented the detailed experimental data of the crosswind condition, air temperature distribution inside and outside of the NDDCT and the cooling performance. The experimental data demonstrate the substantial yet complex impact of the crosswind on cooling performance, and significant non-uniformities in air and hot water temperature distributions and strong air vortices inside the tower were observed in high crosswind speeds.

In this study, an inlet cover is proposed to improve the performance of small NDDCTs in crosswinds. CFD analyses of a small NDDCT with tower inlet covers of different lengths were performed. The CFD results presented in this paper provide guidance for small NDDCT design in the future.

2. Numerical model

2.1 Governing equations

The commercial software Ansys/Fluent 15.0 [33] was used in this study. An incompressible air model with a constant density was assumed and Boussinesq's approximation was used to reflect the buoyancy effect caused by density difference [34]. The airflow momentum and turbulence were modelled using the realizable *k-ε* model because it is one of the most appropriate viscous models for low Reynolds numbers [30]. The model was simulated by solving a series of conservation equations of physical quantities, whose general terms are expressed as

$$\nabla.\left(\rho\vec{v}\phi - \Gamma_{\phi}\nabla\phi\right) = S_{\phi} \quad (1)$$

The expressions of ϕ, Γ_{ϕ} and S_{ϕ} for Equation (1) are provided in Table 1. All numerical calculations of the conservation equations were run by using the pressure-based steady-state solver with SIMPLE segregated algorithms and second-order discretization [34].

Table 1 Summary of governing equations

	Φ	S_{ϕ}	Γ_{ϕ}
Continuity	1	0	0
x momentum	U	$-\frac{\partial p}{\partial x} + \nabla\left(\mu_e \frac{\partial \vec{v}}{\partial x}\right) + F_x$	μ_e

y momentum	V	$-\frac{\partial p}{\partial y}+\nabla\left(\mu_e\frac{\partial \vec{v}}{\partial y}\right)-\rho_0\beta(T-T_0)g+F_y$	μ_e
z momentum	W	$-\frac{\partial p}{\partial z}+\nabla\left(\mu_e\frac{\partial \vec{v}}{\partial z}\right)+F_z$	μ_e
Energy	T	$\frac{1}{c_p}(\frac{qA_c}{V_c})$	$\frac{K_e}{c_p}$
Turbulent energy	K	$G_k+G_b-\rho\varepsilon$	$\mu+\frac{\mu_t}{\sigma_k}$
Energy dissipation	ε	$\rho C_1 S\varepsilon+C_{1\varepsilon}C_{3\varepsilon}G_b\frac{\varepsilon}{k}-C_2\rho\frac{\varepsilon^2}{k+\sqrt{v\varepsilon}}$	$\mu+\frac{\mu_t}{\sigma_\varepsilon}$

where

$\mu_e=\mu+\mu_t;\ \mu_t=C_\mu\rho\frac{k^2}{\varepsilon};\ K_e=K+K_t;\ K_t=\frac{c_p\mu_t}{Pr_t};$

$\mathrm{G_k}=\ \mu_{\mathrm{t}}\mathrm{S}^2;\ G_b=\beta g\frac{\mu_t}{Pr_t}\frac{\partial T}{\partial y};\ \beta=\frac{1}{T_0}\Big|p_0;$

$C_1=max\left[0.43,\frac{S_\varepsilon^k}{S_\varepsilon^k+5}\right];\ C_{1\varepsilon}=1.44;\ C_2=1.92;\ \ C_{3\varepsilon}=tanh(\frac{V}{U});\ \ \sigma_k=1.0;\ \ \sigma_\varepsilon=1.44$

$Pr=0.74;\ \ Pr_t=0.85;\ \ T_0=293.15;$

2.2 Computational geometry, boundary conditions and operating parameters

The small NDDCT used by Li et al. [30] was considered in this paper. The NDDCT has a hyperbolic shape, is 20 m high, and has a radius of 6.2625 m. The tower is constructed with a steel truss and PVC membrane. Figure 1 shows the CFD tower model, which has the same geometric dimensions as the small NDDCT considered by Li et al. [30]. The lengths of the tower inlet cover considered in the CFD model are 0 m, 1.5 m, 3 m and 4.5 m. The computational domain (to simulate outside ambient air) is of cylindrical shape, with a radius of 72 m and height of 120 m, as previous CFD studies have shown that the distances from the tower to the domain boundaries do not affect the numerical results when the domain diameter is 12 times the tower diameter and the domain height is 6 times the tower height [28].

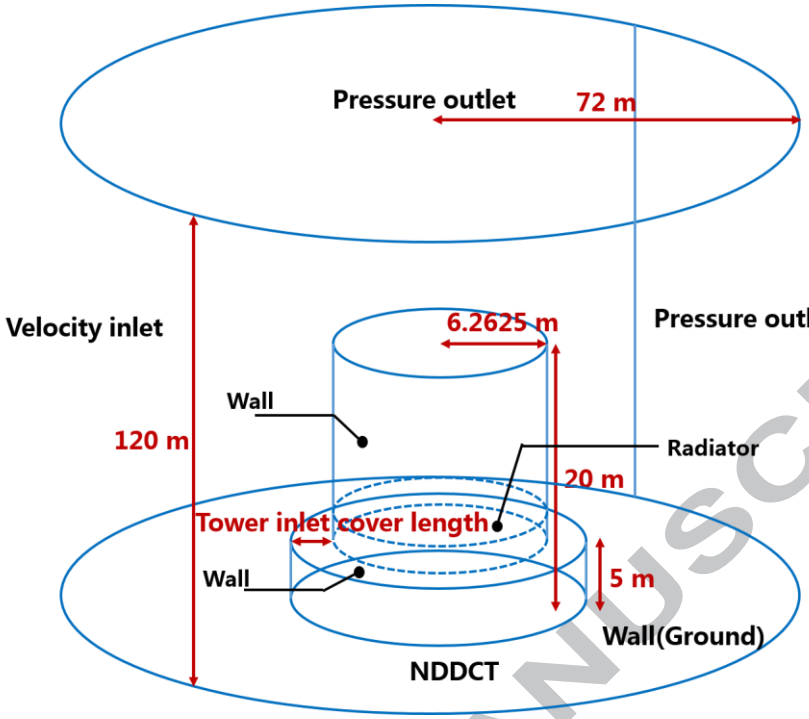

Figure 1 Computational geometry of the small NDDCT

The 'ground' in the CFD domain, the 'wall' in the tower and the tower inlet cover are set as the non-slip and zero heat flux 'wall' boundary. The top and leeward side of the domain are set as the 'pressure outlet' boundary. The inlet air temperature is set to the NDDCT's design air temperature (303.15 K) [30]. The windward side of the domain is set as the 'velocity inlet' boundary [28]. The velocity profile is defined by Eq.(2), where a is recommended as 0.2 [23].

$$\frac{v_{dt,cw}}{v_{dt,ref}} = \left(\frac{y}{y_{ref}}\right)^{a} \tag{2}$$

Several ways of modelling heat exchangers in CFD can be found in open literature. The radiator model in Ansys/Fluent is used to calculate the performance of the air-cooled heat exchanger of the cooling tower [35]. The heat transfer in the heat exchanger can be presented by the following equation:

$$q_{dt} = h_{dt}\left(T_{dt,r} - T_{dt,a2}\right) \tag{3}$$

Where the heat transfer coefficient, h_{dt}, is a function of the heat exchanger characteristic parameters and the air inlet velocity. $T_{dr,r}$ is the radiator temperature and $T_{dt,a2}$ is the air temperature downstream of the radiator [28].

For air flow pressure drop, the radiator model can simulate resistance to air flow in

the direction normal to radiator face. However, it does not provide resistance in other two directions, i.e. velocity components parallel to radiator face. This will cause overestimation of the possibility of vertices occurring near the radiator, since real structure of fin tube heat exchanger bundles can prevent horizontal air flow, allowing air flow through heat exchanger only vertically. Therefore a porous media model is added to represent the pressure loss within the heat exchanger, leaving the radiator model to represent heat transfer only [28]. The pressure drop of the heat exchanger bundles is modelled by porous zone through adding a momentum source term into the corresponding equation [9]. As presented in Eq.(4), the source term is composed by two parts: a viscous loss term and an inertial loss term.

$$F_i = -\left(\frac{\mu_e}{\alpha} v_i + C\frac{1}{2}\rho {v_i}^2\right) \tag{4}$$

Where α and C are determined by the friction factor of heat exchangers in the NDDCT 1D model [28].

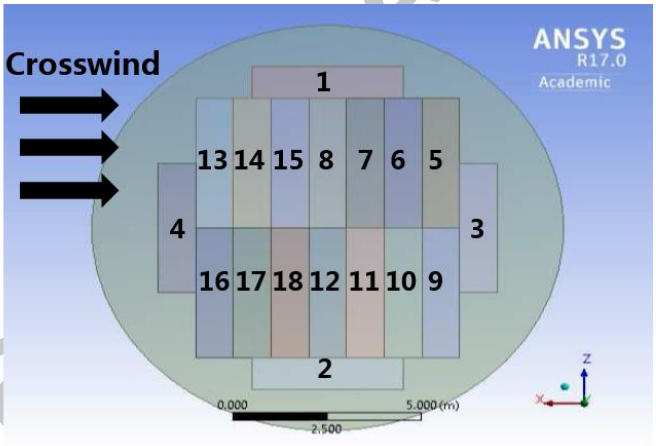

Figure 2 Heat exchangers in the NDDCT

All 18 heat exchanger bundles are horizontally arranged inside the NDDCT [30]. These heat exchanger bundles cover 70% of the cross-sectional surface area. The 18 heat exchanger bundles are built separately in the CFD model, and their locations are the same as those in the NDDCT [30], as shown in Figure 2. The number of each heat exchanger bundle and the direction of the crosswind are also shown in Figure 2.

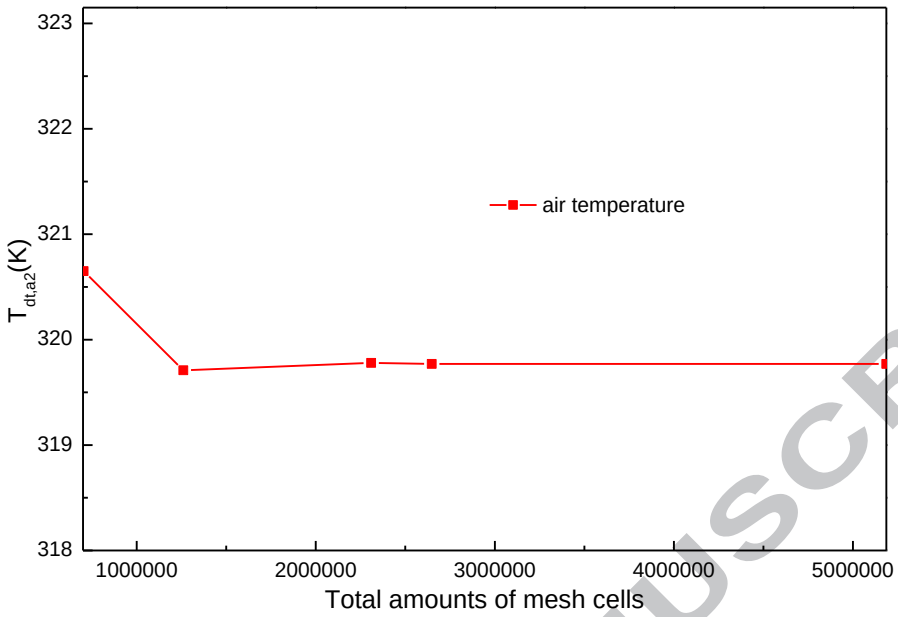

(a) Tower outlet air temperature

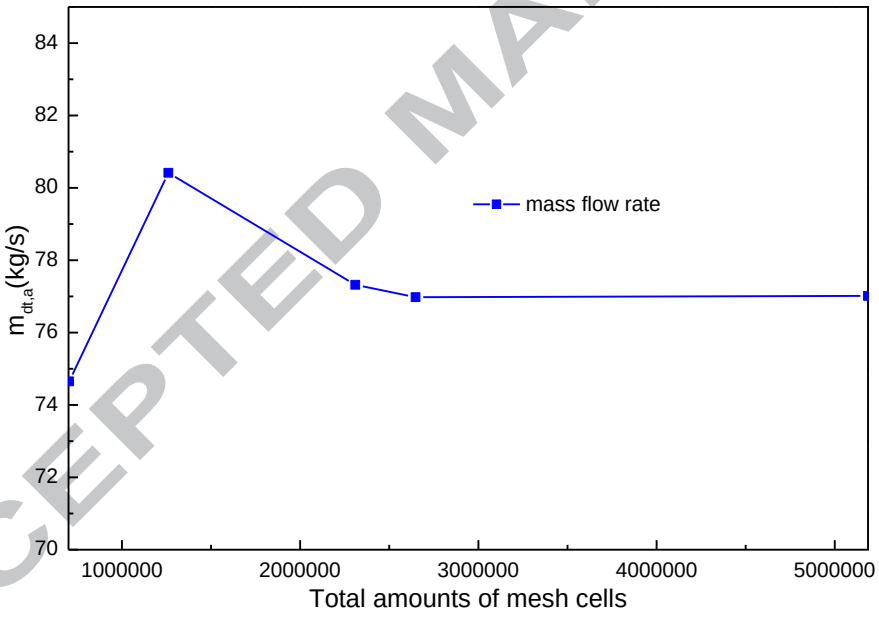

(b) Tower outlet air mass flow rate

Figure 3 Grid independence test

The cooling tower and the heat exchanger bundles are discretised by the structured hexahedron mesh, adopting the ANSYS meshing sweep method. The mesh of the computation domain area is generated using the ANSYS meshing multi-zone method [30]. The results of the grid independence test shown in Figure 3 show that the deviations in

the tower outlet air temperature and tower outlet air mass flow rate are only 0.001 K and 0.03 kg/s, respectively, when there are 2,647,840 and 5,186,700 mesh cells. Thus, 2,647,840 cells are used in this paper.

3. Model validation

3.1 Scaled NDDCT experiment

3.1.1 Windless condition

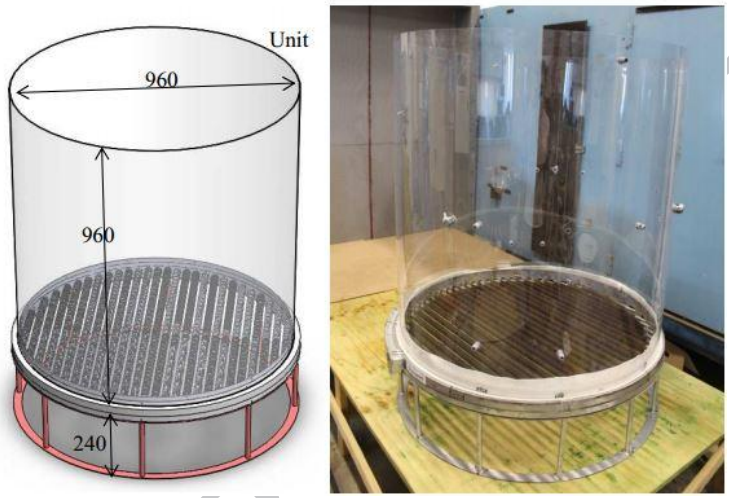

Figure 4 Scaled NDDCT used by Lu et al. [29]

Lu et al. [29] used a 1:12.5-scale cooling tower model equipped with an electric resistance heater simulating horizontally placed heat exchangers to validate the CFD model. The experiment was performed in an open circuit wind tunnel. The scaled experimental model had a height of 1.2 m and diameter of 0.96 m, as shown in Figure 4. The CFD model built in this paper is the same size as the tower. A grid with 2,121,255 cells was used. The details of the CFD model are provided in Ref [29].

The mean tower outlet air velocity ($v_{dt,a2}$) and air temperature ($T_{dt,a2}$) were measured in the experiment [29]. A direct comparison of the results of the measurement [29] and the CFD model is provided in Table 2, showing the good agreement between them.

Table 2 Comparison of the CFD results and experiment results [29]

Parameters	Measurement [29]	CFD results	Deviation
$V_{dt,a2}$(m/s)	0.32	0.31	3.1%
$T_{dt,a2}$(K)	316.45	315.65	1.8%

3.1.2 Crosswind condition

Figure 5 Air flow inside the scaled NDDCT under crosswind conditions [29]

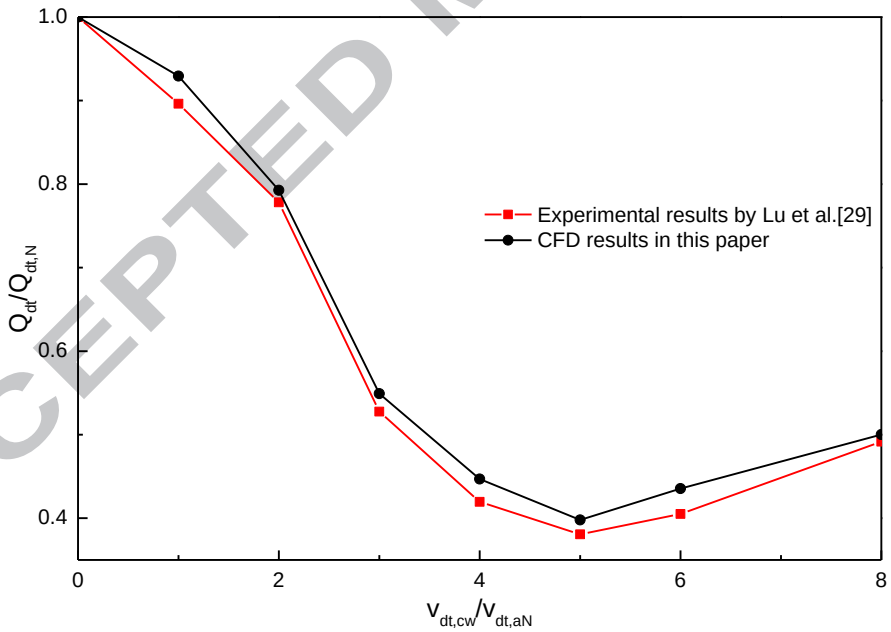

Figure 6 Comparison of the CFD results and experimental results [29]

Lu et al. [29] also performed an experiment to study the tower performance with a crosswind, as shown in Figure 5. A comparison with CFD models shows the good agreement of the experimental and numerical results when the conditions of the CFD

model and the experimental model are similar. In this paper, a CFD simulation was conducted to enable a comparison with the experimental results. The results are shown in Figure 6. The results show that the model corresponds well with the experimental results of the scaled tower [29].

3.2 Full-scale NDDCT experiment

The CFD method used in this paper is also validated based on the full-scale tests on the same cooling tower [32]. The results show that the air flow behavior inside the NDDCT under crosswind condition can be well presented by the CFD modeling. The numerical results can be well matched with the experimental measurements.

4. Results and discussions

4.1 Flow and temperature fields

4.1.1 Tower inlet cover length of 0 m

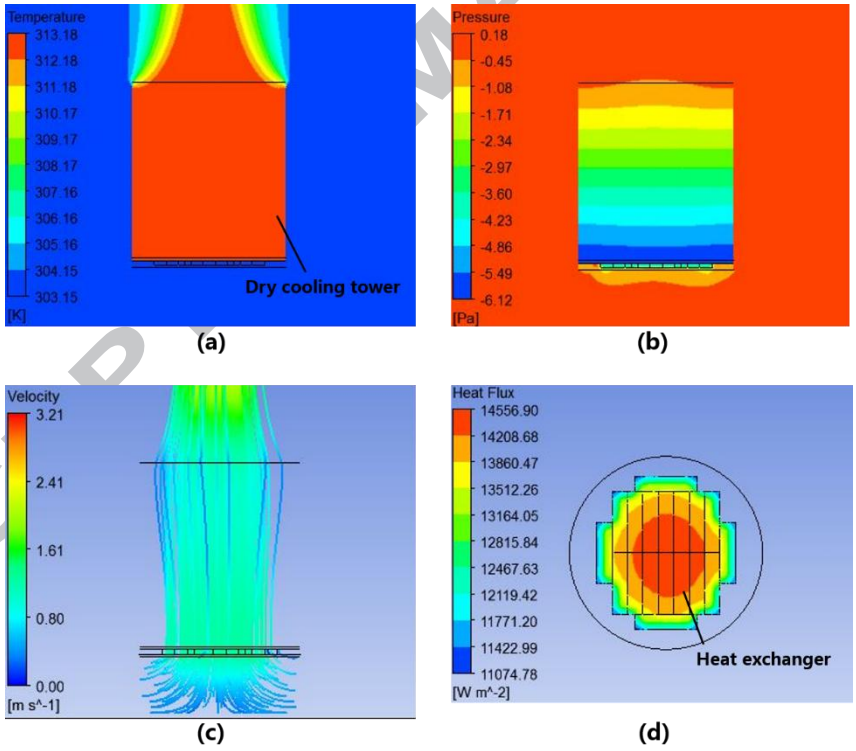

Figure 7 Tower performance

(Tower inlet cover length = 0 m, crosswind speed = 0 m/s)

(a) air temperature, (b) air pressure, (c) air flow, (d) heat flux

Due to the central symmetry of configurations of heat exchangers and the NDDCT, the temperature, pressure, flow and heat flux fields exhibit central symmetry characteristics in the absence of a crosswind, as shown in Figure 7. With no crosswind, heat is mainly transferred from cooling water to air through natural convection heat transfer in the NDDCT. The air temperature above the heat exchangers is around 313.18 K. Figure 7 (b) shows that negative pressure is formed inside the tower, which is caused by the balance between the buoyancy force and viscous force. The largest pressure difference could reach around 6.3 Pa. The pressure difference inside and outside the tower sucks air into the tower. Figure 7 (c) shows that the air flow near the edge of the heat exchangers is smaller than that at the tower centre due to the higher air resistance. As a result, the heat flux of the heat exchangers at the edge of the tower is smaller than that at the tower centre (Figure 7 (d)).

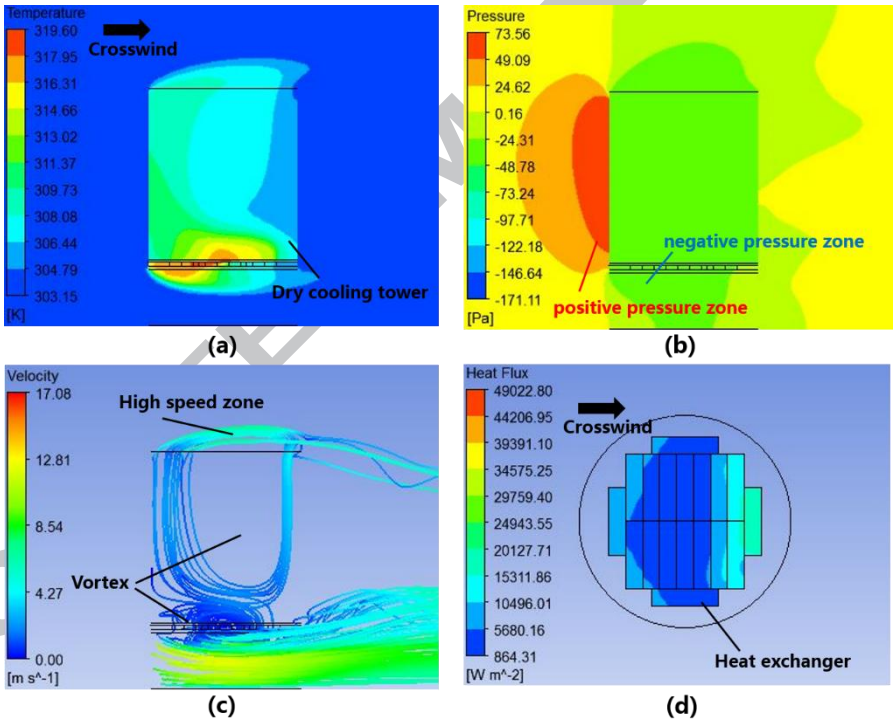

Figure 8 Tower performance

(Tower inlet cover length = 0 m, crosswind speed = 10 m/s)

(a) air temperature, (b) air pressure, (c) air flow, (d) heat flux

Figure 8 shows that the temperature, pressure, flow and heat flux fields inside the tower are no longer symmetrical when the crosswind speed is 10 m/s. In contrast to the

windless condition in Figure 7, heat is transferred from cooling water to air through natural convection heat transfer and forced convection heat transfer under crosswind conditions [9]. Figure 8 (a) shows that the air temperature at the tower's windward side is higher than that at the leeward side. This trend is due to the change in the flow field inside the tower (Figure 8(c)) resulting from the crosswind. According to Figure 8 (b), a negative pressure zone is formed beneath the heat exchangers on the windward side. The negative pressure zone decreases the pressure difference between the inside and outside of the tower, which causes the lower air flow through the windward side than through the leeward side. This lower air flow inevitably increases the air temperature on the windward side. A comparison of Figures 7 (d) and 8 (d) illustrates that the heat flux of the heat exchangers on the tower leeward side increases from around 12000 W/m^2 to over 20000 W/m^2. By contrast, the heat flux on the windward side decreases significantly with a crosswind. Figure 8(c) shows that the upper vortex caused by a crosswind forms a high-speed zone that acts as a lid above the tower outlet, making it more difficult for air to leave the tower [28].

Figure 9 shows the velocity vectors in the xy plane when the crosswind speed is 10 m/s. According to Figure 8(b), the crosswind creates a high-pressure zone because it is blocked by the tower side wall. This high-pressure zone pushes the air at the tower side wall into the tower inlet, which acts as a lid, as shown by the blue arrow in Figure 9. This situation makes it difficult for air to enter the heat exchangers at the tower windward side because of the inertia effect even though the tower's draft continues to suck air in. The black dashed line in Figure 9 illustrates that air would eventually enter the tower through this route. Thus, a negative pressure zone under the heat exchangers at the tower windward side and a vortex at the bottom of the tower would inevitably form, leading to a decrease in air flow through the heat exchangers, as shown in Figure 8(b), (c) and Figure 9. Therefore, the high-pressure zone around the tower side wall is the reason for the formation of the negative pressure zone under the heat exchangers on the tower windward side, the vortex at the bottom of the tower, reducing air flow through the tower.

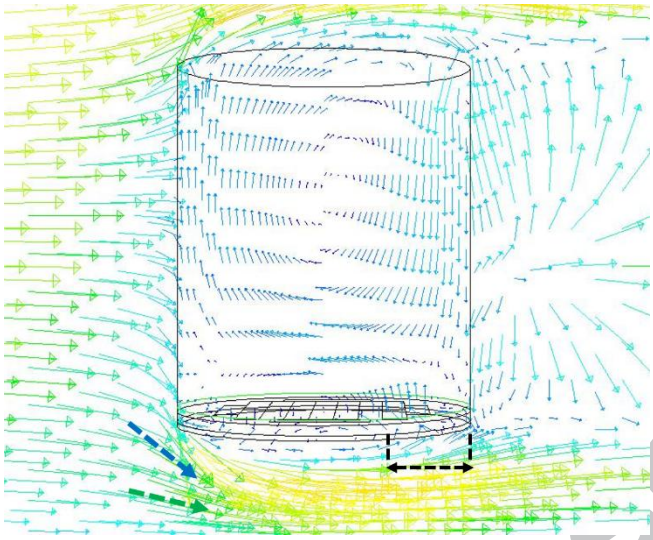

Figure 9 Velocity vectors in the xy plane

(Tower inlet cover length = 0 m, crosswind speed = 10 m/s)

4.1.2 Tower inlet cover length of 1.5 m

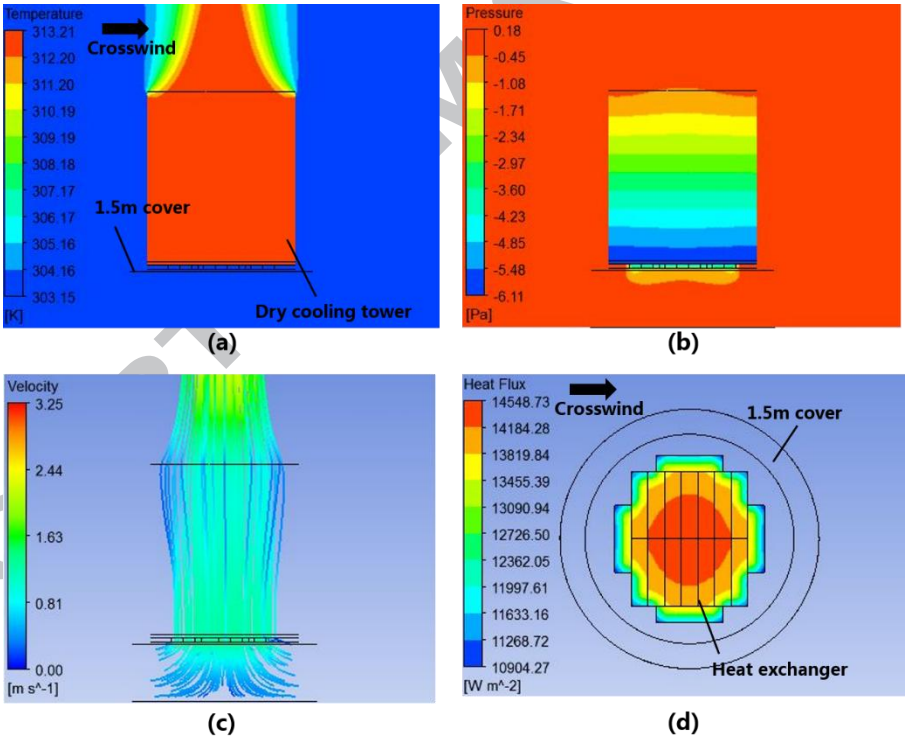

Figure 10 Tower performance

(Tower inlet cover length = 1.5 m, crosswind speed = 0 m/s)

(a) air temperature, (b) air pressure, (c) air flow, (d) heat flux

Figure 10 shows the temperature, pressure, flow and heat flux fields inside the tower

when the length of the tower inlet cover is 1.5 m and the crosswind speed is 0 m/s. Compared with Figure 7, Figure 10 shows that the 1.5 m tower inlet cover has a negligible influence on the tower performance under windless conditions. Figures 7 (d) and 10(d) illustrate that the impact of the cover on the heat exchangers' heat flux is also small.

Figure 11 shows the temperature, pressure, flow and heat flux fields inside the tower when the length of the tower inlet cover is 1.5 m and the crosswind speed is 10 m/s. Figures 11(c) and 8(c) illustrate that the 1.5 m tower inlet cover reduces the impact of the vortex inside the tower and increases the air flow through the tower, thus improving the heat flux of the heat exchangers at the tower centre and leeward sides.

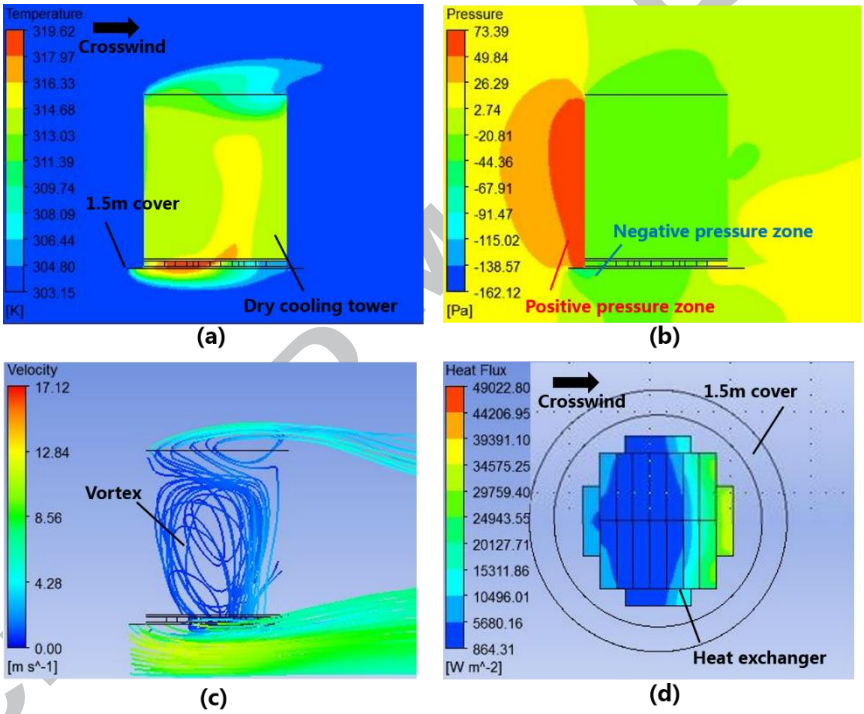

Figure 11 Tower performance

(Tower inlet cover length = 1.5 m, crosswind speed = 10 m/s)

(a) air temperature, (b) air pressure, (c) air flow, (d) heat flux

4.1.3 Tower inlet cover length of 3 m

Figure 12 shows the temperature, pressure, flow and heat flux fields inside the tower when the length of the tower inlet cover is 3 m and the crosswind speed is 10 m/s. Figures 12(a) and 8(a) illustrate that the 3 m tower inlet cover reduces the area of high air

temperature on the tower windward side. In addition, the negative pressure zone area is also decreased, causing a significant rise in the air flow through the tower. A comparison of Figures 12(d) and 8(d) illustrates that the 3 m tower inlet cover substantially improves the heat flux of all heat exchangers except those on the tower windward side. The tower thermal performance is also improved.

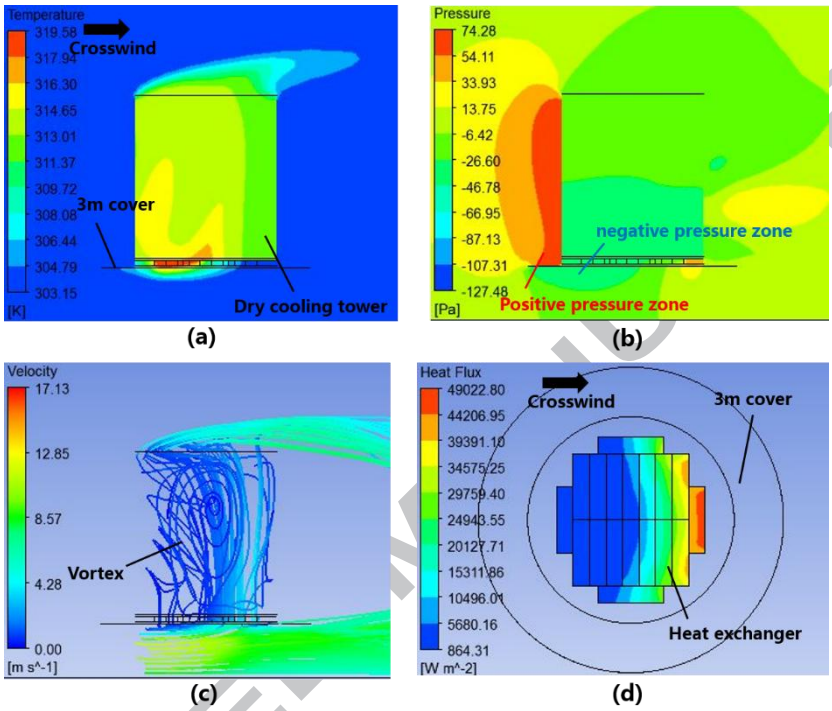

Figure 12 Tower performance

(Tower inlet cover length = 3 m, crosswind speed = 10 m/s)

(a) air temperature, (b) air pressure, (c) air flow, (d) heat flux

Figure 13 shows the air velocity vectors in the xy plane with the 3 m tower inlet covers when the crosswind speed is 10 m/s. Based on the discussion in Section 4.1.1, the high-pressure zone around the tower side wall causes the formation of the negative pressure zone under heat exchangers on the tower windward side, the vortex at the bottom of the tower, reducing air flow through the tower. As shown in Figure 9, when the tower inlet cover is 0 m, the high-pressure zone around the tower side wall pushes air into the tower through the black dashed line. Figure 13 shows that a remarkable high-pressure zone also forms outside the tower when the tower inlet cover is 3 m. However, the 3 m tower inlet cover prevents the majority of the crosswind around the tower side wall from

entering the tower inlet, and only a small amount of crosswind changes flow direction, acting as a lid, as shown by the blue arrow in Figure 13. The slope of the blue arrow in Figure 13 is smaller than that in Figure 9 because of the weaker impact of crosswind around the tower inlet on the flow direction. The heat exchanger area that air flows through is enlarged by installing the 3 m tower inlet cover. Thus, the tower inlet cover improves the tower performance with a crosswind by reducing the impact of the high-pressure zone around the tower side wall.

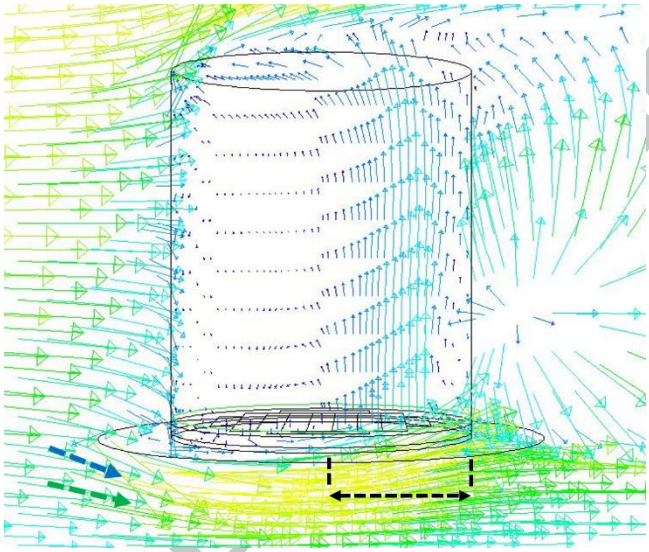

Figure 13 Velocity vectors in the xy plane

(Tower inlet cover length = 3 m, crosswind speed = 10 m/s)

4.1.4 Tower inlet cover length of 4.5 m

Figure 14 shows the temperature, pressure, flow and heat flux fields inside the tower when the length of the tower inlet cover is 4.5 m and the crosswind speed is 10 m/s. Figures 8, 11, 12 and 14 illustrate that the air temperature distribution inside the tower becomes more homogeneous as the length of the tower inlet cover increases from 0 m to 4.5 m. In addition, the negative pressure zone area under the heat exchangers is also decreased continuously, causing an increase in air flow through the tower. When the length of the tower inlet cover increases to 4.5 m, the heat flux distribution in the heat exchangers becomes more homogeneous and the heat flux in most heat exchangers increases significantly.

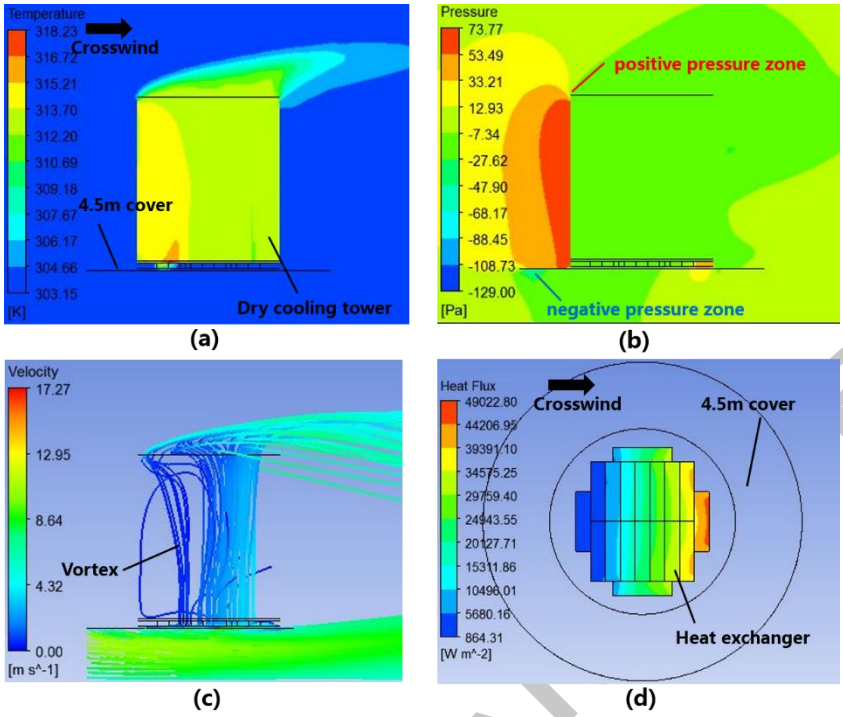

Figure 14 Tower performance

(Tower inlet cover length = 4.5 m, crosswind speed = 10 m/s)

(a) air temperature, (b) air pressure, (c) air flow, (d) heat flux

4.2 Thermal Performance

Figure 15 shows the performance of the heat exchangers with different crosswind conditions when the length of the tower inlet cover is 0 m. The zig zag change of the curves in Figure 15 reveals the variation in the performance of heat exchangers arranged in different locations, as shown in Figure 2. For heat exchangers #1 and 2 located at the two sides of the tower, the air flow rate and heat flux decrease continuously from around 5 kg/s to around 0.5 kg/s and from around 50 kW/m^2 to around 15 kW/m^2 respectively, as the crosswind increases from 0 m/s to 6 m/s; when the crosswind increases to 6 m/s, the direction of air flow through these two heat exchangers reverses and the air flow becomes negative because of the vortex at the bottom of the tower (Figure 8(c)); the air flow and heat flux increase as the crosswind increases from 6 m/s to 12 m/s. For heat exchanger #3 on the tower leeward side, the air flow and heat flux increase continuously when crosswind increases from 0 m/s to 6 m/s; the air flow and heat flux suddenly decrease to their minimum values (around 5 kg/s and 45 kW/m^2) when the crosswind increases to 8

m/s; and the air flow and heat flux again increase as the crosswind increases from 8 m/s to 12 m/s.

For heat exchanger #4 on the tower windward side, the sudden decrease of the air flow and heat flux under 2 m/s crosswind condition is because of the sudden appearance of the vortex at the bottom of the tower under crosswind conditions. With the increase of the crosswind, the direction of air flow reverses due to the vortex at the bottom of the tower; the air flow and heat flux increase as the crosswind increases from 4 m/s to 12 m/s. This is due to the growing impact of the vortex at the bottom of the tower with the increasing crosswind (Figure 8(c)).

For heat exchangers #5, 6, 9 and 10, air flow and heat flux rise to their maximum values as the crosswind increases from 0 m/s to 4 m/s; the air flow and heat flux decease to their minimum values as the crosswind increases from 4 m/s to 8 m/s; and the air flow and heat flux again increase when the crosswind increases from 8 m/s to 12 m/s. For heat exchangers #7, 8, 11 and 12 arranged at the tower centre, the air flow and heat flux decrease continuously as the crosswind increases from 0 m/s to 6 m/s, and the air flow and heat flux remain approximately stable as the crosswind increases from 6 m/s to 12 m/s. For heat exchanges #13, 14, 15, 16, 17 and 18 arranged on the tower windward side, the air flow and heat flux both decrease as the crosswind increases from 0 m/s to 2 m/s; and the vortex at the bottom of the tower reverses air flow direction as the crosswind increases from 2 m/s to 12 m/s, causing the air flow and heat flux to increase.

Figure 16 shows the performance of the heat exchangers with different crosswinds when the length of the tower inlet cover is 4.5 m. For heat exchangers #1 and 2 located at the sides of the tower, the air flow and heat flux increase with an increase in crosswind from around 5 kg/s to around 10.5 kg/s and from around 50 kW/m^2 to around 95 kW/m^2. For heat exchangers #3, 5, 6, 7, 8, 9, 10, 11 and 12 arranged on the tower leeward side, the air flow and heat flux increase with increases in the crosswind, but the increment in air flow and heat flux decreases with decreases in the distance between the heat exchanger and tower centre. For heat exchangers #4, 13, 14, 15, 16, 17 and 18 arranged on the tower windward side, the air flow and heat flux decrease with increases in the crosswind.

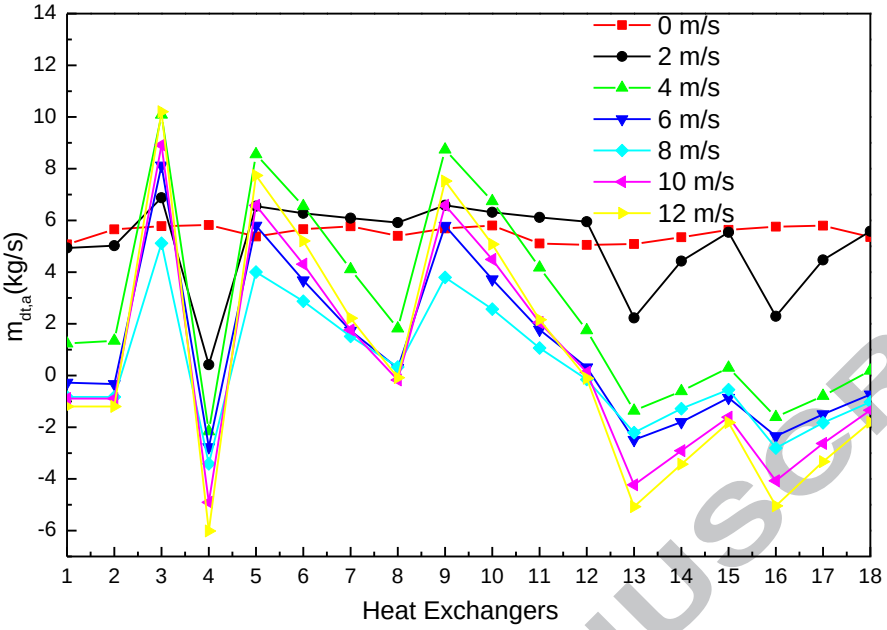

(a) Air flow

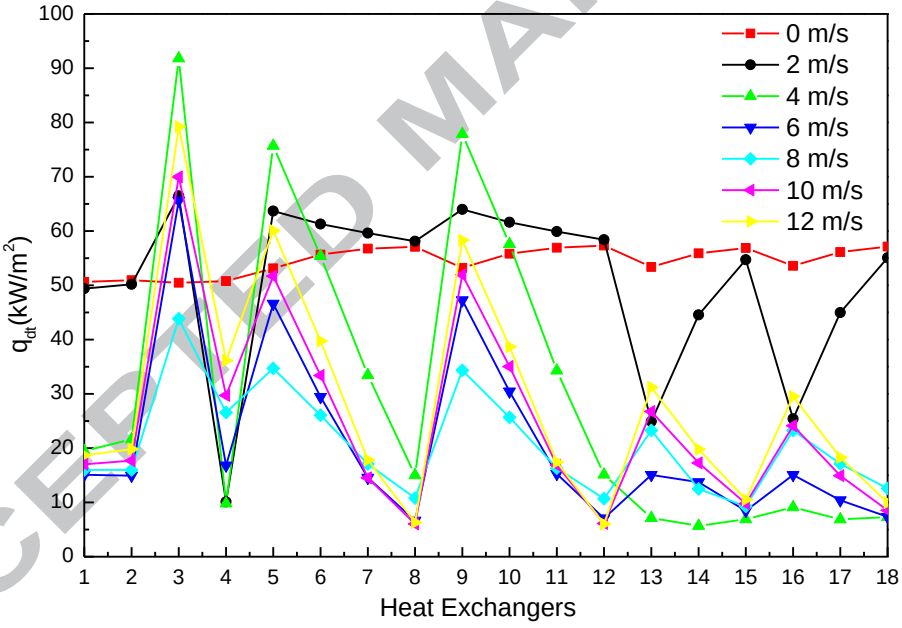

(b) Heat flux

Figure 15 Performance of the heat exchangers with different crosswinds

(Tower inlet cover length = 0 m)

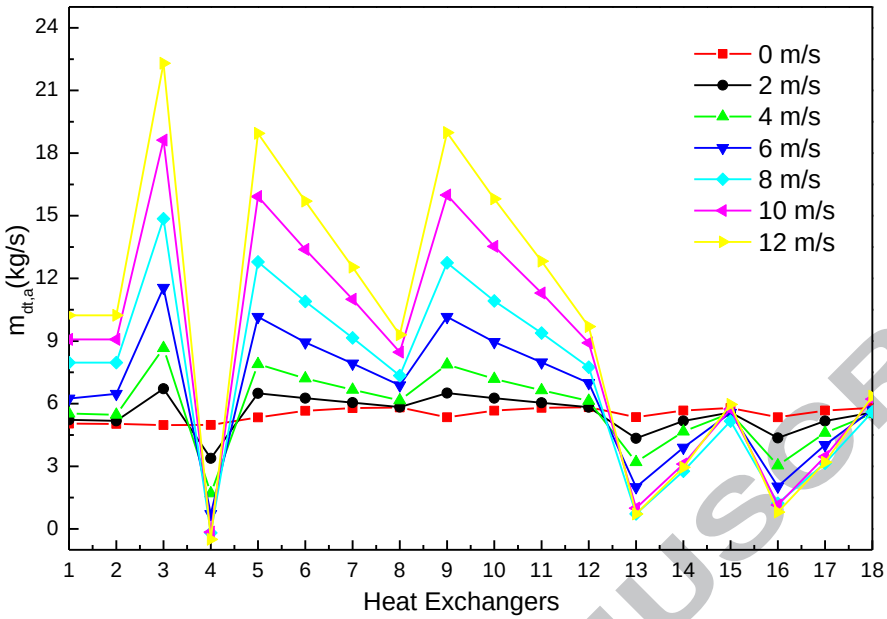

(a) Air flow

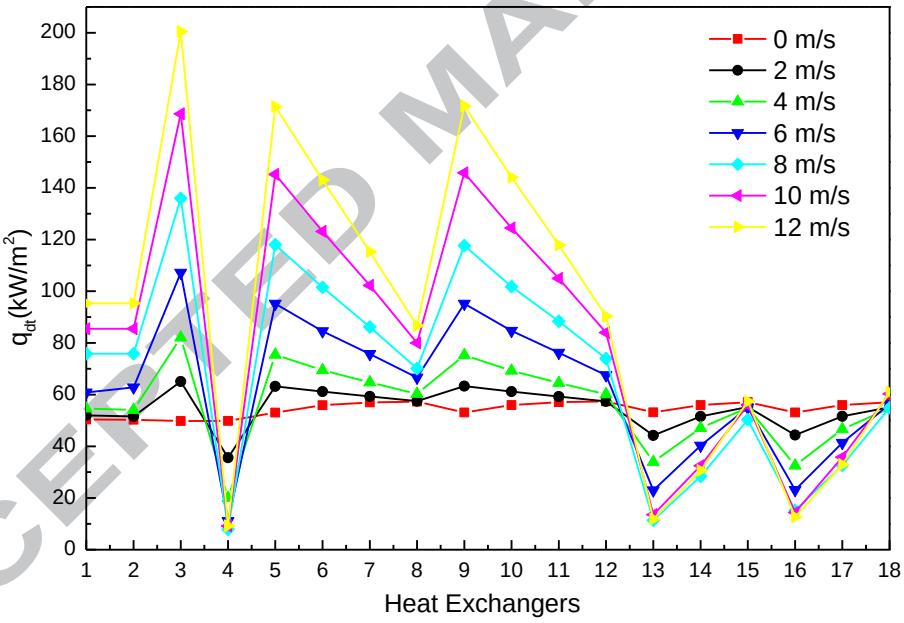

(b) Heat flux

Figure 16 Performance of the heat exchangers with different crosswinds

(Tower inlet cover length = 4.5 m)

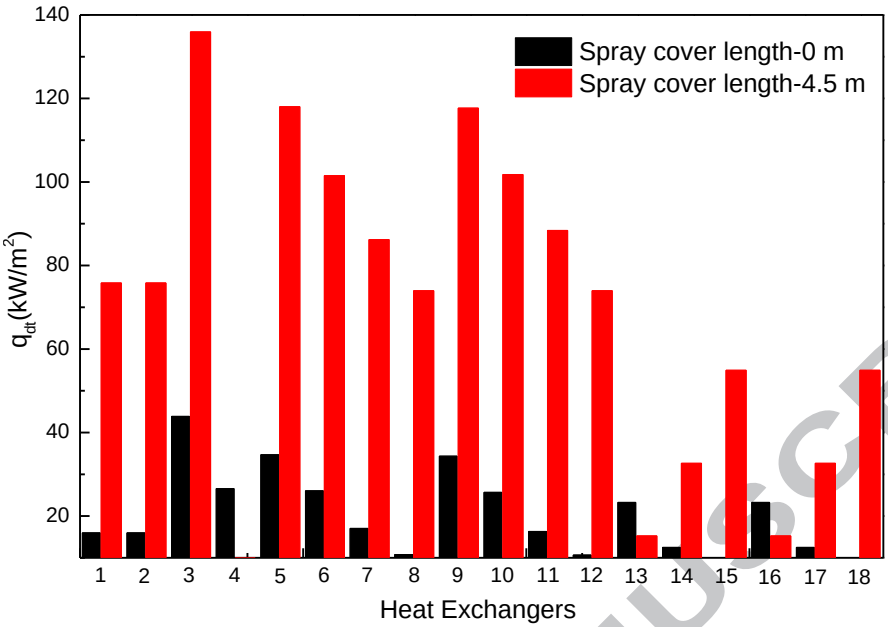

Figure 17 Performance of each heat exchanger with an 8 m/s crosswind (Tower inlet cover length = 0 m, 4.5 m)

Figure 17 shows a comparison of each heat exchanger's heat flux with two different tower inlet cover lengths when the crosswind is 8 m/s. The heat flux in all heat exchangers except #4, 13 and 16 increases tremendously when the crosswind is 8 m/s. The largest increase in the heat flux could be found in heat exchangers #8 and 12. The value rises almost 7 times from around 11 kW/m^2 to around 74 kW/m^2.

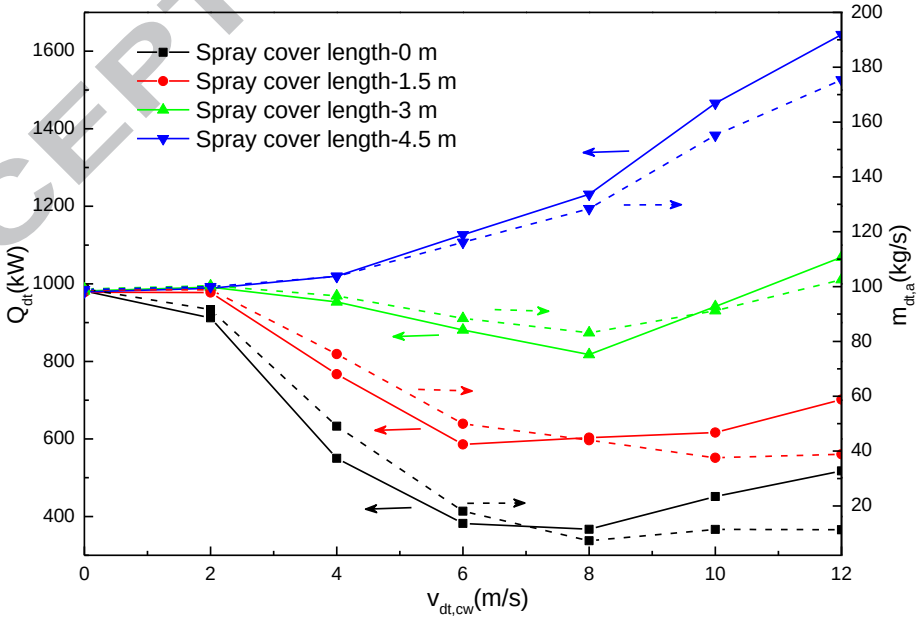

Figure 18 Comparison of the tower performance with different crosswind conditions

The tower performance with different crosswinds and different tower inlet covers is shown in Figure 18. When the length of the tower inlet cover is 0 m, the tower heat load and air flow decrease significantly as the crosswind increases from 0 m/s to 8 m/s; the tower heat load with a 8 m/s crosswind is approximately 40% of the value with no crosswind (367 kW VS. 982 kW). As the crosswind continues to increase, the air flow remains nearly stable but the tower heat load increases. Lu et al. [29] researched this phenomenon and found that it was caused by the transfer of the heat inside the dry cooling tower to air through natural convection heat transfer and the forced convection heat transfer with the crosswind. The forced convection heat transfer is calculated by the equation $Nu = \frac{h_T d_o}{k} = 0.495 {Re_c}^{0.509} \left(\frac{P_t}{d_o}\right)^{-0.209}$, where Re_c depends on the crosswind. Although natural convection heat transfer decreases with increasing crosswind, the forced convection heat transfer increases with increasing crosswind. When the crosswind is larger than 8 m/s, the increment in forced convection heat transfer is larger than the decrement in the natural convection heat transfer, and the tower overall heat load increases. The trend of the crosswind influence on tower performance with the 1.5 m tower inlet cover is the same as that with the 0 m tower inlet cover. When the crosswind increases, the tower heat load and air flow initially decrease and then increase. However, the 1.5 m tower inlet cover significantly improves tower performance with a crosswind. When the crosswind increases from 4 m/s to 12 m/s, the tower heat load increases by 40-65% when installing the 1.5 m tower inlet cover. When the crosswind is 8 m/s, the tower heat load and air flow when installing 1.5 m tower inlet cover are 603 kW and 44 kg/s. In contrast, the values are only 367 kW and 7 kg/s without tower inlet cover. The tower performance can be further improved by installing the 3 m tower inlet cover. The tower heat load reaches its lowest value when the crosswind increases to 8 m/s, approximately 83% of the value with no crosswind. When the crosswind continuously increases to 12 m/s, the tower heat load surpasses the value with no crosswind. In general, the tower heat load improves by 70-130% when installing the 3 m tower inlet cover when the crosswind increases from 4 m/s to 12 m/s. When the tower inlet cover is 4.5 m, crosswind is no longer a factor leading to deterioration in tower performance. In contrast, the cover

improves the tower heat load and air flow considerably; when the crosswind reaches 12 m/s, the tower heat load is 68% greater than that with no crosswind (1642 kW VS. 980 kW). When the crosswind increases from 4 m/s to 12 m/s, the tower performance increases by 85-230% with the installation of the 4.5 m tower inlet cover.

5 Conclusion

Crosswind creates a high-pressure zone, which pushes the air at the NDDCT side wall into the tower inlet. This crosswind acts as a lid, making it difficult for air to enter the heat exchangers on the tower windward side because of the inertia effect even though the tower draft continues to suck air in. A negative pressure zone forms under the heat exchangers on the tower windward side, and a vortex forms at the bottom of the tower, leading to a decrease in air flow through the heat exchangers and a deterioration in tower performance.

The tower inlet cover prevents the majority of the crosswind around the tower side wall from entering the tower inlet, reducing the negative impact of the high-pressure zone around the tower side wall on the tower performance. The air flow at the heat exchangers is increased, which significantly improves the heat flux of the heat exchangers except for those on the tower windward side. The thermal performance of the tower is also improved.

When the crosswind increases from 4 m/s to 12 m/s, the 1.5 m tower inlet cover improves the tower heat load by 40-65%. The 3 m tower inlet cover improves the tower heat load by 70-130%, and the 4.5 m tower inlet cover improves the tower heat load by 85-230%. When the tower inlet cover length is 4.5 m, crosswind is no longer a factor leading to a deterioration in tower performance; in contrast, the cover increases the tower heat load and air flow considerably under crosswind conditions.

6 Acknowledgements

The authors gratefully acknowledge the funding support from the Fundamental Research Funds for the Central Universities (Grant No. 2017QNA07).

List of symbols and acronyms

A_c surface area of numerical cell (m^2)

a constant

C inertial resistance factor

C_1, $C_{1\varepsilon}$, C_2, $C_{3\varepsilon}$ constants in turbulent equations

C_p specific heat ($J.kg^{-1}\ K^{-1}$)

$C\mu$ coefficient in trubulent viscosity

F source term for momentum equations

G_b turbulent kinetic energy source term due to buoyancy

G_k turbulent kinetic energy source term due to mean velocity gradients

H height (m)

h convective heat transfer coefficient ($W.m^{-2}\ K^{-1}$)

K, K_e, K_t laminar, effective, turbulent thermal conductivity repectively ($W.m^{-1}\ K^{-1}$)

K_{resist} pressure loss coefficient

k turbulent kinetic energy ($m^2.s^{-2}$)

NDDCT natural draft dry cooling tower

NDWCT natural draft wet cooling tower

N_u Nusselt number

Pr, Pr_t laminar, turbulent Prandtl number, respectively (m)

p pressure (Pa)

Q heat transfer rate (kW)

q heat flux($kW.m^{-2}$)

S modulus of the mean rate-of-strain tensor

S_φ volumetric source term for variable quantity ϕ

T temperature (K)

U, V, W velocity components in x-, y-, z-direction ($m.s^{-1}$)

Vc numerical cell volume (m^3)

v velocity scalar ($m.s^{-1}$)

x, y, z Cartesian co-ordinates

Greek letters

α permeability (m^2)

β bulk thermal expansion coefficient (K^{-1})

ε turbulent kinetic energy dissipation ($m^2.s^{-3}$)

ϕ scalar quantity ($u,v,w,T,k,\ \varepsilon,....$)

Γ_φ diffusion coefficient for variable quntitty ϕ

ρ density , mean density ($kg.m^{-3}$)

μ, μ_e, μ_t laminar, effective, turbulent viscosity, respectively ($kg.m^{-1}\ s^{-1}$)

σk, $\sigma\varepsilon$ turbulent Prandtl number for k and ε, respectively

Subscripts

a *air*

cw crosswind condition

*d*t dry cooling tower

N pure natural convection case

r radiator

ref reference value

1,2 inside or inlet, outside or outlet

Reference

[1] S.V. Bedekar, P. Nithiarasu, K.N. Seetharamu, Experimental investigation of the performance of a counter-flow, packed-bed mechanical cooling tower, Energy 23 (11) (1998) 943-947.

[2] M. Lemouari, M. Boumaza, I.M. Mujtaba, Thermal performances investigation of a wet cooling tower, Applied Thermal Engineering 27 (5) (2007) 902-909.

[3] K. Singh, R. Das, A feedback model to predict parameters for controlling the performance of a mechanical draft cooling tower, Applied Thermal Engineering 105 (2016) 519-530.

[4] K. Singh, R. Das, An improved constrained inverse optimization method for mechanical draft cooling towers, Applied Thermal Engineering 114 (2017) 573-582.

[5] L. Xia, D. Liu, L. Zhou, F. Wang, P. Wang, Optimal number of circulating water pumps in a nuclear power plant, Nuclear Engineering and Design 288 (2015) 35-41.

[6] C.R. Williams, M.G. Rasul, Feasibility of a hybrid cooling system in a thermal power plant, Proceedings of the 3rd Iasme/Wseas International Conference on Energy & Environment (2008) 124-129.

[7] H. Gurgenci, Fresh water using geothermal heat, Australasian Science 31 (5) (2010) 35-37.

[8] L. Xia, J. Li, W. Ma, H. Gurgenci, Z. Guan, P. Wang, Water Consumption Comparison Between a Natural Draft Wet Cooling Tower and a Natural Draft Hybrid Cooling Tower—An Annual Simulation for Luoyang Conditions, Heat Transfer Engineering 38 (11-12) (2017) 1034-1043.

[9] X. Li, Z. Guan, H. Gurgenci, Y. Lu, S. He, Simulation of the UQ Gatton natural draft dry cooling tower, Applied Thermal Engineering 105 (2016) 1013-1020.

[10] R.V. Rao, V.K. Patel, Optimization of mechanical draft counter flow wet-cooling tower using artificial bee colony algorithm, Energy Conversion and Management 52 (7) (2011) 2611-2622.

[11] A. Alkhedhair, H. Gurgenci, I. Jahn, Z. Guan, S. He, Numerical simulation of water spray for pre-cooling of inlet air in natural draft dry cooling towers, Applied Thermal Engineering 61 (2) (2013) 416-424.

[12] A. Alkhedhair, I. Jahn, H. Gurgenci, Z. Guan, S. He, Parametric study on spray cooling system for optimising nozzle design with pre-cooling application in natural draft dry cooling towers, International Journal of Thermal Sciences 104 (2016) 448-460.

[13] A. Alkhedhair, I. Jahn, H. Gurgenci, Z. Guan, S. He, Y. Lu, Numerical simulation of water spray in natural draft dry cooling towers with a new nozzle representation approach, Applied Thermal Engineering 98 (2016) 924-935.

[14] L. Xia, H. Gurgenci, D.Y. Liu, Z.Q. Guan, L. Zhou, P. Wang, CFD analysis of pre-cooling water spray system in natural draft dry cooling towers, Applied Thermal Engineering 105 (2016) 1051-1060.

[15] S. He, Z. Guan, H. Gurgenci, K. Hooman, Y. Lu, A. M. Alkhedhair, Experimental study of the application of two trickle media for inlet air pre-cooling of natural draft dry cooling towers, Energy Conversion and Management 89 (2015) 644-654.

[16] S. He, Z. Guan, H. Gurgenci, I. Jahn, Y. Lu, A. M. Alkhedhair, Influence of ambient conditions and water flow on the performance of pre-cooled natural draft dry cooling towers, Applied Thermal Engineering 66 (1–2) (2014) 621-631.

[17] S. He, H. Gurgenci, Z. Guan, X. Huang, M. Lucas, A review of wetted media with potential application in the pre-cooling of natural draft dry cooling towers, Renewable and Sustainable Energy Reviews 44 (2015) 407-422.

[18] A.F. du Preez, D.G. Kröger, The effect of the heat exchanger arrangement and wind-break walls on the performance of natural draft dry-cooling towers subjected to cross-winds, Journal of Wind Engineering and Industrial Aerodynamics 58 (3) (1995) 293-303.

[19] R. Al-Waked, M. Behnia, The effect of windbreak walls on the thermal performance of natural draft dry cooling towers, Heat Transfer Engineering 26 (8) (2005) 50-62.

[20] M. Goodarzi, A proposed stack configuration for dry cooling tower to improve cooling efficiency under crosswind, Journal of Wind Engineering and Industrial Aerodynamics 98 (12) (2010) 858-863.

[21] M. Goodarzi, R. Keimanesh, Heat rejection enhancement in natural draft cooling tower using radiator-type windbreakers, Energy Conversion and Management 71 (2013) 120-125.

[22] M. Goodarzi, R. Ramezanpour, Alternative geometry for cylindrical natural draft cooling tower with higher cooling efficiency under crosswind condition, Energy Conversion and Management 77 (2014) 243-249.

[23] L.J. Yang, X.P. Wu, X.Z. Du, Y.P. Yang, Dimensional characteristics of wind effects on the

performance of indirect dry cooling system with vertically arranged heat exchanger bundles, International Journal of Heat and Mass Transfer 67 (2013) 853-866.

[24] L. Chen, L. Yang, X. Du, Y. Yang, Performance improvement of natural draft dry cooling system by interior and exterior windbreaker configurations, International Journal of Heat and Mass Transfer 96 (2016) 42-63.

[25] H. Ma, F. Si, Y. Kong, K. Zhu, W. Yan, Wind-break walls with optimized setting angles for natural draft dry cooling tower with vertical radiators, Applied Thermal Engineering 112 (2017) 326-339.

[26] W. Wang, J. Lyu, H. Zhang, Q. Liu, G. Yue, W. Ni, A performance enhancement of a natural draft dry cooling tower in crosswind via inlet flow field reconstruction, Energy and Buildings 164 (2018) 121-130.

[27] Y. Kong, W. Wang, X. Huang, L. Yang, X. Du, Annularly arranged air-cooled condenser to improve cooling efficiency of natural draft direct dry cooling system, International Journal of Heat and Mass Transfer 118 (2018) 587-601.

[28] Y. Lu, Z. Guan, H. Gurgenci, Z. Zou, Windbreak walls reverse the negative effect of crosswind in short natural draft dry cooling towers into a performance enhancement, International Journal of Heat and Mass Transfer 63 (2013) 162-170.

[29] Y. Lu, Z. Guan, H. Gurgenci, K. Hooman, S. He, D. Bharathan, Experimental study of crosswind effects on the performance of small cylindrical natural draft dry cooling towers, Energy Conversion and Management 91 (2015) 238-248.

[30] X. Li, L. Xia, H. Gurgenci, Z. Guan, Performance enhancement for the natural draft dry cooling tower under crosswind condition by optimizing the water distribution, International Journal of Heat and Mass Transfer 107 (2017) 271-280.

[31] X. Li, S. Duniam, H. Gurgenci, Z. Guan, A. Veeraragavan, Full scale experimental study of a small natural draft dry cooling tower for concentrating solar thermal power plant, Applied Energy 193 (2017) 15-27.

[32] X. Li, H. Gurgenci, Z. Guan, X. Wang, S. Duniam, Measurements of crosswind influence on a natural draft dry cooling tower for a solar thermal power plant, Applied Energy 206 (2017) 1169-1183.

[33] Fluent, Ansys Fluent Theory Guide, 14.0 ed., ANSYS, Inc., 2011.

[34] Y. Lu, H. Gurgenci, Z. Guan, S. He, The influence of windbreak wall orientation on the cooling performance of small natural draft dry cooling towers, 79(2014) 1059-1069.

[35] C.J. Zhao, J.W. Han, X.T. Yang, J.P. Qian, B.-L. Fan, A review of computational fluid dynamics for forced-air cooling process, Applied Energy 168 (2016) 314-331.

Highlights

1. A cover to improve the NDDCT performance under crosswind conditions is presented.
2. The impact of crosswind on vortex formation inside NDDCT is explained.
3. The working mechanism of the cover and its effects are presented.
4. 4.5 m cover improves the tower heat load by 85-230% under crosswind conditions.